Progress In Electromagnetics Research Letters, Vol. 112, 111–118, 2023

Modeling of TSV-Based 3-D Heterogeneous Solenoid Inductor with High Inductance Value

Jinrong Su[1, *], Haobo Wang[1], Haipeng Dou[2], and Xinwei Chen[1]

Abstract—In this letter, a novel 3-D heterogeneous solenoid inductor with high inductance value is proposed. By adding planar spiral structure at the ends of through-silicon vias (TSVs) of typical 3-D solenoid inductor, the heterogeneous solenoid is formed. The total inductance is increased by more than 41% compared with that of typical solenoid inductor of the same size. Additionally, an accurate analytical model of the inductor is established considering all the factors including angle and offset. Q3D simulation results verified the accuracy of the model, and the percentage error is less than 5.38%. This work provides an important reference for inductor designers to quickly estimate inductance value, configuration, and layout area.

1. INTRODUCTION

With the development of miniaturization of wireless communication system, higher requirements are put forward for fully integrated technology. As a necessary component of energy storage and filtering, the integration of inductors is a key technology that restricts the full integration of a radio frequency (RF) system [1]. Small occupation area, high inductance, and high Q have always been the pursuit of inductor designers [2]. The 3-D solenoid inductor based on through-silicon via (TSV) technology has been proved to be one of the most effective solutions to improve integration and performance. A great deal of research has been done on its modeling and optimization. For example, in terms of inductor modeling, [3] proposed a simple electrical model of 3-D solenoid inductor using data fitting method but lack of physical interpretation. In [4], a circuit model of TSV-based solenoid inductor was proposed considering both temperature and geometrical parameters. Moreover, [5] put forward a simple and accurate analytical model with an error of less than 7.5%. To improve the model accuracy in [5], both internal inductance and details of redistribution layer inductance were considered in [6]. Besides, [7] established physics-based modeling of 3-D inductor considering skin and proximity effects, making it suitable broadband estimation. In addition to modeling, the optimization of inductor structure has also been carried out. For instance, ground shielding TSVs were added around the TSV-based solenoid inductor to suppress the crosstalk in [8]. An equivalent model was also established considering the ground TSVs, and the error is less than 5%. [9] proposed a nested solenoid inductor based on TSV, which promoted inductance value dramatically. The works above provide important basis and reference for future research. It is worth noting that in many applications the required inductance value is so rigorous that only adjusting multiple parameters comprehensively can obtain ideal value. Simple methods need to be studied. Furthermore, how to promote inductance value in limited area is still worth further exploration.

In this letter, a 3-D heterogeneous solenoid (HS) inductor structure is proposed. A planar spiral structure is added to introduce horizontal magnetic flux. As a result, the inductance value is increased

Received 18 July 2023, Accepted 18 September 2023, Scheduled 2 October 2023

* Corresponding author: Jinrong Su (sujinrong@sxu.edu.cn).

[1] School of Physics and Electronic Engineering, Shanxi University, Shanxi 030006, China. [2] School of Information Engineering, Shanxi Vocational University of Engineering Science and Technology, Jinzhong, China.

dramatically. Besides, the inductance value can be fine-tuned by changing number of planar spiral structures without adjusting the entire structure. Additionally, the equivalent electrical model is established for quick estimation of the inductance value and occupied area of the inductor. The accuracy of the model is verified against the Q3D simulation results, and the error is less than 5.38%.

2. CONFIGURATION OF THE HS INDUCTOR

2.1. Typical Structure

Figure 1(a) shows the schematic of a typical TSV-based solenoid inductor. The tracks in the redistribution layer (RDL) are connected to the vertical TSVs in the silicon substrate to form a solenoid structure. For an N-turn HS inductor, there are $2N$ TSVs arranged in N rows and 2 columns.

2.2. Heterogeneous Solenoid Inductor

To increase the total length of the inductor metal track and introduce magnetic flux across the horizontal plane simultaneously, planar spiral structures are added at ends of TSV to form a heterogeneous solenoid (HS) inductor. Take 4-turns as an example, as illustrated in Fig. 1(b), planar spiral structures are alternately connected to the top or bottom of TSVs. Alternating arrangement is aimed at reducing the capacitance effect. In order to facilitate elaboration, the 4-turns HS inductor with geometric parameters listed in Table 1 is taken as the instance below.

Figure 2 depicts the inductance value of the proposed HS inductors and the typical ones for different turn numbers, N. Identical substrate and geometric parameters are set when calculating. It is clear that the value of both structures increases with N, and the value of the HS inductor is larger. For

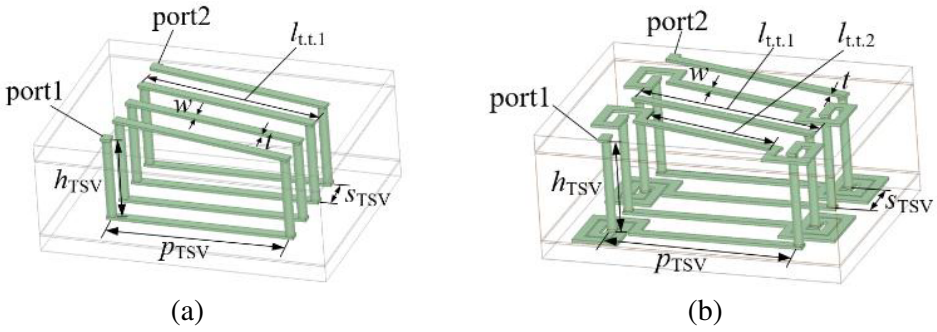

Figure 1. Configurations of 3-D solenoid inductor: (a) typical and (b) proposed HS inductor.

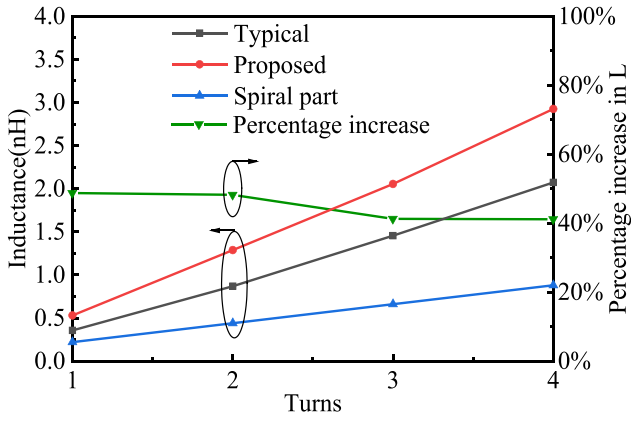

Figure 2. Comparison of inductance value between the HS inductors and typical ones.

Table 1. Geometric parameters of the HS inductor.

Symbol	Design parameters	Value/μm
p_{TSV}	TSV pitch	200
s_{TSV}	TSV spacing	40
h_{TSV}	TSV height	100
r_{TSV}	TSV radius	5
d_{RDL}	Distance between top and bottom RDL tracks	103
$l_{\mathrm{b.t.}}$	Bottom RDL track length	176
$l_{\mathrm{t.t.1}}$	Top layer type 1 track length	204
$l_{\mathrm{t.t.2}}$	Top layer type 2 track length	174
s	Slot width of bottom spiral	2
w	RDL track width	10
t_{RDL}	RDL track thickness	3
r_{in}	Top spiral inner diameter	15

example, when N is 3, the inductance value of typical inductor is 1.46 nH while that of the HS inductor is 2.06 nH. Besides, the inductance of the spiral structure is plotted, and it is seen that it contributes a lot to the promotion of the total inductance. More than 41% is increased by adding the spiral structures.

3. INDUCTANCE MODELING

The inductance value of the HS inductor is the total of the self-inductance and mutual inductance of TSV, RDL tracks, and planar spirals. The inductance modeling of each part is established in detail below.

3.1. Inductance Modeling of TSVs

A single TSV can be regarded as a cylindrical metal, and its self-inductance can be calculated by [6]:

$$L_{\mathrm{self}}(h_{\mathrm{TSV}}, r_{\mathrm{TSV}}) = \frac{\mu_0 h_{\mathrm{TSV}}}{2\pi}\left[\ln\frac{2h_{\mathrm{TSV}}}{r_{\mathrm{TSV}}} - 1 + \frac{r_{\mathrm{TSV}}}{h_{\mathrm{TSV}}}\right] + \frac{\mu_0 h_{\mathrm{TSV}}}{8\pi} \tag{1}$$

where $\mu_0 = 4\times10^{-7}$ H/m is the vacuum permeability, and $\mu_0 h_{\mathrm{TSV}}/8\pi$ is the internal inductance of TSV. There are $2N$ TSVs in N-turns solenoid inductor. Thus, the total self-inductance of TSVs can be expressed as

$$L_{\mathrm{TSV,self}} = 2NL_{\mathrm{self}}\left(h_{\mathrm{TSV}}, r_{\mathrm{TSV}}\right) \tag{2}$$

To calculate mutual inductance between TSVs, the distances between different TSVs, d, need to be clarified first. For the i-th and j-th TSVs in the same column that are not adjacent, d is denoted by $d_{\mathrm{TSV.s.c.}}$, and it equals ks_{TSV}, where $k = |i-j|$. For TSVs in different rows and different columns, d equals $[p_{\mathrm{TSV}}^2 + (ks_{\mathrm{TSV}})^2]^{1/2}$, and it is denoted by $d_{\mathrm{TSV.d.c.}}$. The mutual inductance between two TSVs with the distance of d can be calculated by [7]

$$M_{\mathrm{align}}(h_{\mathrm{TSV}}, d) = \frac{\mu_0}{2\pi}\left[h_{\mathrm{TSV}}\sinh^{-1}\frac{h_{\mathrm{TSV}}}{d} - \sqrt{h_{\mathrm{TSV}}^2 + d^2} + d\right] \tag{3}$$

By replacing d in the formula with s_{TSV}, $d_{\mathrm{TSV.s.c.}}$, or $d_{\mathrm{TSV.d.c.}}$, the mutual inductance between each two TSVs in the HS inductor can be obtained. The currents flowing through TSVs in the same column are in the same direction, and that in different columns are reversed. The total mutual inductance between TSVs in the same columns can be described by

$$M\left(h_{\mathrm{TSV}}, d_{\mathrm{TSV,s.c.}}\right) = 2\sum_{m=1}^{N-1}\left(N-m\right)M_{\mathrm{align}}\left(h_{\mathrm{TSV}}, ms_{\mathrm{TSV}}\right), \tag{4}$$

and that in different columns can be expressed as

$$M\left(h_{\mathrm{TSV}}, d_{\mathrm{TSV,d.c.}}\right) = NM_{\mathrm{align}}\left(h_{\mathrm{TSV}}, p_{\mathrm{TSV}}\right) + 2\sum_{k=1}^{N-1}\left(N-k\right)M_{\mathrm{align}}\left(h_{\mathrm{TSV}}, d_{\mathrm{TSV,d.c.}}\right) \tag{5}$$

Since the mutual inductance between TSVs with the same currents' direction is positive and that with opposite direction is negative, the total inductance of TSVs is

$$L_{\mathrm{TSV,sum}} = 2NL_{\mathrm{self}}\left(h_{\mathrm{TSV}}, r_{\mathrm{TSV}}\right) + 2\left[M\left(h_{\mathrm{TSV}}, d_{\mathrm{TSV,s.c.}}\right) - M\left(h_{\mathrm{TSV}}, d_{\mathrm{TSV,d.c}}\right)\right] \tag{6}$$

3.2. Inductance Modeling of RDL Tracks

Similarly, both self-inductance and mutual inductance between different tracks in RDLs should be considered when the inductance model of RDL tracks is established. Let's start with the self-inductance calculation. There are three different lengths of tracks. The bottom RDL tracks have the same length of $l_{\mathrm{b.t.}} = p_{\mathrm{TSV}} - 2s - 2w$, and two adjacent tracks are offset, as shown in yellow rectangles in Fig. 3. Besides, the top tracks have two lengths, $l_{\mathrm{t.t.1}}$ and $l_{\mathrm{t.t.2}}$. The self-inductance of each track can be obtained by replacing h_{TSV} with the track lengths and r_{TSV} with $w/2$ in formula (1). Then the total self-inductance of the tracks in both layers can be obtained as

$$\begin{aligned} L_{\mathrm{RDL,self}} &= mL_{\mathrm{self}}\left(l_{\mathrm{t.t.1}}\right) + mL_{\mathrm{self}}\left(l_{\mathrm{t.t.2}}\right) + 2mL_{\mathrm{self}}\left(l_{\mathrm{b.t.}}\right), \ N \text{ is even}, \ m = \frac{N}{2} \\ L_{\mathrm{RDL,self}} &= mL_{\mathrm{self}}\left(l_{\mathrm{t.t.1}}\right) + \left(m+1\right)L_{\mathrm{self}}\left(l_{\mathrm{t.t.2}}\right) + \left(2m+1\right)L_{\mathrm{self}}\left(l_{\mathrm{b.t.}}\right), \ N \text{ is odd}, \ m = \frac{N-1}{2} \end{aligned} \tag{7}$$

where $l_{\mathrm{t.t.1}} = [(p_{\mathrm{TSV}})^2 + (s_{\mathrm{TSV}})^2]^{1/2}$, and $l_{\mathrm{t.t.2}} = [(p_{\mathrm{TSV}})^2 + (s_{\mathrm{TSV}})^2]^{1/2} - 2r_{\mathrm{in}}$.

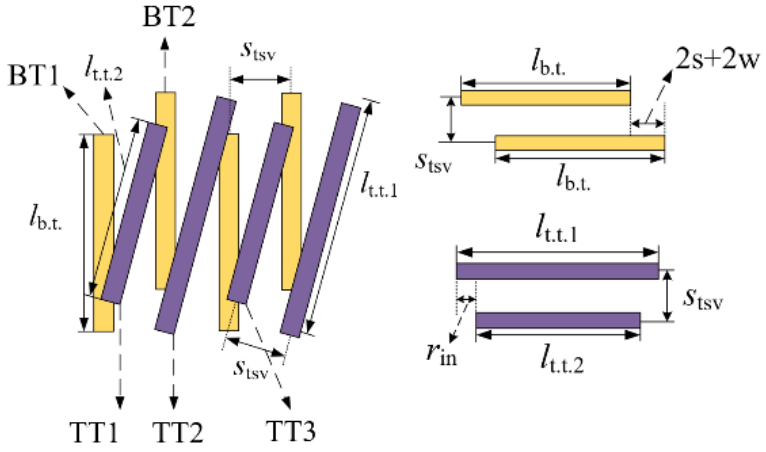

Figure 3. Top view of RDL tracks. The tracks in yellow are in bottom layer and that in purple are in top layer.

For two tracks that are both in odd (or even) rows in the bottom layer, their ends are aligned. Thus, the mutual inductance can be calculated by replacing h_{TSV} with $l_{\mathrm{b.t.}}$ and r_{TSV} with $w/2$ in formula (3). For two tracks that one is in odd (or even) row and the other in even (or odd) row, their ends are staggered by $2s - 2w$. The mutual inductance can be calculated using (3) [10]

$$M_{\mathrm{offset,bot}} = M_{\mathrm{align}}\left(p_{\mathrm{TSV}}, d_{ij}\right) + M_{\mathrm{align}}\left(p_{\mathrm{TSV}} - 2s - 2w, d_{ij}\right) - 2M_{\mathrm{align}}\left(2s + 2w, d_{ij}\right), \tag{8}$$

where d_{ij} is the distance between two tracks. The total mutual inductance between tracks in bottom layer is

$$\begin{aligned} M_{\mathrm{RDL,bot}} \ = \ & 2\sum_{m=1}\left[\left(N-2m\right)M_{\mathrm{align}}\left(l_{\mathrm{b.t.}}, 2ms_{\mathrm{TSV}}\right)\right] \\ & +2\sum_{m=1}\left[\left(N-\left(2m-1\right)\right)M_{\mathrm{offset,bot}}\left(l_{\mathrm{b.t.}}, \left(2m-1\right)s_{\mathrm{TSV}}\right)\right], \ m = 1, 2, ... \frac{N}{2} \text{ or } \frac{N+1}{2}. \end{aligned} \tag{9}$$

Similar to the bottom layer, the top layer tracks that are both in odd (or even) rows are aligned, and the mutual inductance between them can be obtained by replacing parameters in formula (3). The tracks with different lengths are staggered. The mutual inductance between them can be calculated as

$$M_{\text{offset,top}} = 2M_{\text{align}}\left(\sqrt{p_{\text{TSV}}^2 + s_{\text{TSV}}^2} - r_{\text{in}}, d\right) - 2M_{\text{align}}\left(r_{\text{in}}, d\right), \tag{10}$$

where d is the distance between tracks and equals $(2m-1)s_{\text{TSV}}$ ($m = N/2$, $m = 1, 2, 3.....$). The total mutual inductance between the top RDL tracks is obtained as

$$\begin{aligned} M_{\text{RDL,top}} \;=\; & \sum_{k=1}^{m-1} kM_{\text{align}}\left(l_{\text{t.t.1}}, 2\left(m-k\right)s_{\text{TSV}}\right) + \sum_{k=1}^{m-1} kM_{\text{align}}\left(l_{\text{t.t.1}}, 2\left(m-k\right)s_{\text{TSV}}\right) \\ & + \sum_{k=1}^{m}\left[(N-(2k-1))M_{\text{offset,top}}\left((2k-1)\,s_{\text{TSV}}\right)\right] \quad m = \frac{N}{2} \text{ or } \frac{N-1}{2} \end{aligned} \tag{11}$$

As there is an angle θ between the top and bottom tracks, a schematic of layout relationship is plotted in Fig. 4 to clarify the geometric parameters. The dotted line in Fig. 4 shows the projection of the top track on the bottom layer. The extension line of the projection forms an angle θ (equals $\arctan(s_{\text{TSV}}/p_{\text{TSV}})$) with the extension line of the bottom track. Additionally, the lengths of the two extension lines are α and β, and they can be calculated by the trigonometric function. Since the bottom tracks are staggered and the top tracks in different lengths, four different positional relationships should be considered. To illustrate this visually, each track in top layer is labeled as TTi and that in bottom layer labeled as BTi, as shown in Fig. 3. The lengths of α and β for different groups of tracks are listed in Table 2.

Table 2. α and β for different groups of tracks.

α_i	length	β_i	length	Group
α_1	$r_{\text{in}} + 2k[(s_{\text{TSV}})^2 + (p_{\text{TSV}})^2]^{1/2}$	β_1	$2kp_{\text{TSV}}$	BT1 vs TT1
α_2	$2(k-1)[(s_{\text{TSV}})^2 + (p_{\text{TSV}})^2]^{1/2}$	β_2	$2(s+w) + 2(k-1)p_{\text{TSV}}$	BT2 vs TT2
α_3	$(2k-)[(s_{\text{TSV}})^2 + (p_{\text{TSV}})^2]^{1/2}$	β_3	$(2k-1)p_{\text{TSV}}$	BT1 vs TT2
α_4	$r_{\text{in}} + (2k-1)[(s_{\text{TSV}})^2 + (p_{\text{TSV}})^2]^{1/2}$	β_4	$2(s+w) + (2k-1)p_{\text{TSV}}$	BT2 vs TT3

The lengths of the end-to-end connection between the endpoints of the top and bottom tracks are calculated as follows [10]:

$$R_1 = \left[d^2 + (\alpha+l)^2 + (\beta+m)^2 - 2\left(\alpha+l\right)\left(\beta+m\right)\cos\theta\right]^{1/2} \tag{12}$$

$$R_2 = \left[d^2 + (\alpha+l)^2 + \beta^2 - 2\beta\left(\alpha+l\right)\cos\theta\right]^{1/2} \tag{13}$$

$$R_3 = \left[d^2 + \alpha^2 + \beta^2 - 2\alpha\beta\cos\theta\right]^{1/2} \tag{14}$$

$$R_4 = \left[d^2 + \alpha^2 + (\beta+m)^2 - 2\alpha\left(\beta+m\right)\cos\theta\right]^{1/2} \tag{15}$$

Using the geometric parameters calculated above, the mutual inductance can be obtained as [10]:

$$\begin{aligned} M\left(l_{\text{t.t.}}, \alpha, \beta\right) \;=\; & \frac{\mu_0}{2\pi}\cos\theta\Bigg[\left(\alpha + l_{\text{t.t.}}\right)\tanh^{-1}\frac{l_{\text{b.t.}}}{R_1+R_2} + \left(\beta + l_{\text{b.t.}}\right)\tanh^{-1}\frac{l_{\text{t.t.}}}{R_1+R_4} \\ & -\alpha\tanh^{-1}\frac{l_{\text{b.t.}}}{R_3+R_4} - \beta\tanh^{-1}\frac{l_{\text{t.t.}}}{R_2+R_3}\Bigg] - \frac{\mu_0}{4\pi}\frac{\Omega d_{\text{RDL}}}{\tan\theta} \end{aligned} \tag{16}$$

where $l_{\text{t.t.}}$ equals $l_{\text{t.t.1}}$, or $l_{\text{t.t.2}}$. d_{RDL} equals $h_{\text{TSV}} + t_{\text{RDL}}$, and Ω is the solid angle that can be calculated using geometrical parameters including θ, α, β, and tracks lengths [10]. The total mutual inductance

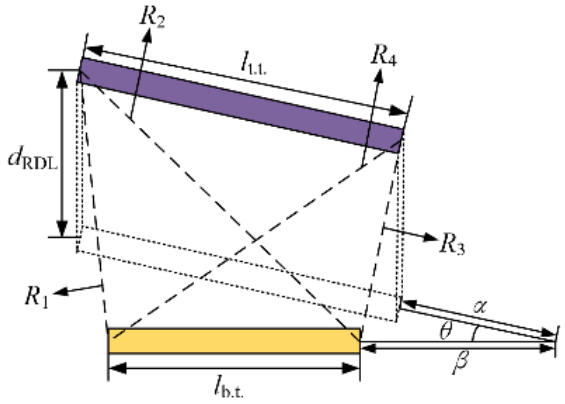

Figure 4. Layout relationship between top track and bottom track.

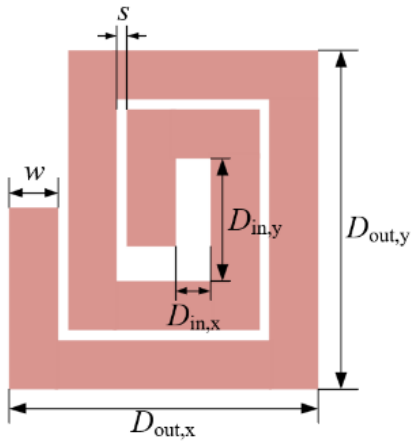

Figure 5. The structure of a 2-turns spiral structure.

between the top and bottom tracks is calculated as

$$M_{\mathrm{RDL,top\_bot1}} = \sum_{k=0}^{m}(N-2k)\,M\left(l_{\mathrm{t.t.2}},\alpha_1,\beta_1\right)+\sum_{k=1}^{m}(N-(2k-1))M\left(l_{\mathrm{t.t.1}},\alpha_2,\beta_2\right) + \sum_{k=1}^{m}(N-(2k-1))M\left(l_{\mathrm{t.t.1}},\alpha_3,\beta_3\right),\ \ m=\frac{N}{2}\ \text{or}\ \frac{N-1}{2} \tag{17-1}$$

$$M_{\mathrm{RDL,top\_bot2}} = 2\sum_{k=1}^{m}(m-k)M(l_{\mathrm{t.t.2}},\alpha_4,\beta_4),\ \ m=\frac{N}{2}\ \text{or}\ \frac{N+1}{2} \tag{17-2}$$

$$M_{\mathrm{RDL,top\_bot}} = M_{\mathrm{RDL,top\_bot1}} + M_{\mathrm{RDL,top\_bot2}} \tag{17}$$

Then, the total inductance of all the RDL tracks is

$$L_{\mathrm{RDL,sum}} = L_{\mathrm{RDL,self}} + M_{\mathrm{RDL,top}} + M_{\mathrm{RDL,bot}} - M_{\mathrm{RDL,top\_bot}} \tag{18}$$

3.3. Inductance Modeling of the Planar Spiral

Figure 5 plots the top view of a planar spiral with inner and outer dimensions $D_{\mathrm{in},x}$, $D_{\mathrm{out},x}$, $D_{\mathrm{in},y}$, $D_{\mathrm{out},y}$, and the mean value in the x and y directions $D_{\mathrm{avg},x}$ and $D_{\mathrm{avg},y}$. The self-inductance $L_{\mathrm{self},x}$, $L_{\mathrm{self},y}$, and mutual inductance M_x, M_y can be calculated using the current sheet approximation method [11]. The total inductance of a planar spiral is

$$L_{\mathrm{spiral}} = 2\left(L_{\mathrm{self},x} + L_{\mathrm{self},y} - M_x - M_y\right) \tag{19}$$

The total inductance $L_{\mathrm{spiral,sum}}$ of the spiral of N-turns solenoid inductor is the sum of all the top spiral inductance $L_{\mathrm{spiral\_top}}$ and the bottom spiral inductance $L_{\mathrm{spiral\_bot}}$:

$$L_{\mathrm{spiral,sum}} = N\left(L_{\mathrm{spiral\_top}} + L_{\mathrm{spiral\_bot}}\right) \tag{20}$$

Since the horizontal part and TSVs are perpendicular to each other, their mutual inductance is zero. The total inductance of the proposed HS inductor is obtained as

$$L_{\mathrm{TOT}} = L_{\mathrm{TSV,sum}} + L_{\mathrm{RDL,sum}} + L_{\mathrm{spiral,sum}} \tag{21}$$

4. VALIDATION AND DISCUSSION

Ansys Q3D was used to verify the accuracy of the proposed theoretical model. In simulation and calculation, the values of h_{TSV}, p_{TSV}, s_{TSV}, and w are set as that listed in Table 1. Fig. 6 compares the simulated and calculated results of L_{TOT} for different h_{TSV}, p_{TSV}, s_{TSV}, and N. N is set to 4 when the other three parameters vary.

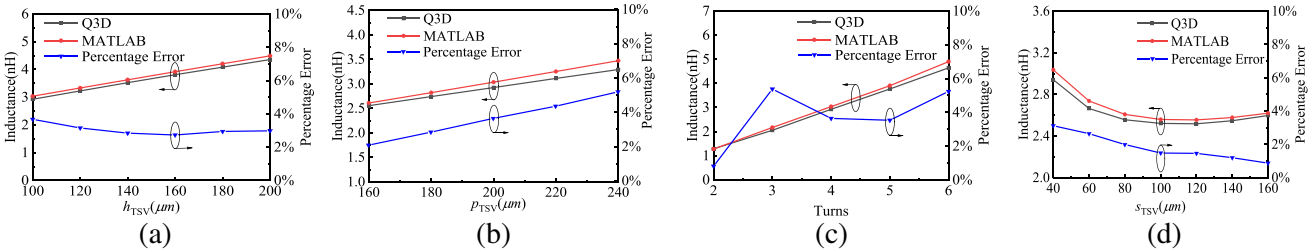

Figure 6. Comparison of inductance value between model calculation and Q3D simulation results for different parameters: (a) h_{TSV}. (b) p_{TSV}. (c) N. (d) s_{TSV}.

The results indicate that the calculated and simulated results agree well over various parameter ranges. The percentage error is less than 5.38%. Besides, L_{TOT} increases with TSV height, TSV pitch, and turn number. The reason is that larger value of those parameters will produce greater self-inductance and mutual inductance according to (1) and (3). Furthermore, in Fig. 6(d), L_{TOT} declines slightly at first but climbs at a certain point as s_{TSV} increases. The reason is that both TSV-to-TSV and track-to-track distances increase with s_{TSV}. According to (3), the mutual inductance decreases. Simultaneously, the length of top RDL tracks increases with s_{TSV}, which will lead to larger inductance. The opposite effect on L_{TOT} forms the curve like a parabola.

Besides, to explore the fine-tuning performance of the HS inductor, Table 3 compares the inductance values of typical inductors with that of the HS inductors added with different planar spiral structures. The parameters of inductors are the same as that in Table 1. As listed in Table 3, the inductance values of the typical inductors are 1.35 nH, 1.83 nH, and 2.32 nH when the turn numbers are 2, 3, and 4, respectively. The inductance value increases by 36.4% and 21.2% by changing the turn number from 2 to 3 and 3 to 4, respectively. It indicates that only changing the turn number cannot achieve values between 1.35 and 1.83 nH (or 1.83 and 2.32 nH). Several parameters must be adjusted comprehensively. In contrast, the inductance values of HS inductor can be fine-tuned by changing the configuration of spiral structures. Take a 3-turns HS inductor as example, the inductance values of 1.87, 1.98, 2.02, and 2.13 nH can be obtained by adjusting number and turns of spiral structures. Compared with the 3-turns typical one, the inductance increases by 2.2%, 8.2%, 10.4%, and 16.4%, respectively. The results indicate that more inductance values can be realized without changing too many structural parameters.

Table 3. Comparison of inductance value of typical and HS inductors.

N	$L_{\mathrm{TOT\_}ty}$/nH	$L_{\mathrm{TOT\_}HS}$			
		$L_{\mathrm{TOT\_1,1}}$	$L_{\mathrm{TOT\_1,2}}$	$L_{\mathrm{TOT\_1,1\&1,2}}$	$L_{\mathrm{TOT\_2,2}}$
2	1.35	1.39	1.50	1.53	1.64
3	1.83	1.87	1.98	2.02	2.13
4	2.32	2.36	2.47	2.51	2.61

$L_{\mathrm{TOT\_}ty}$: Total inductance of typical inductor.
$L_{\mathrm{TOT\_}m,n}$: Total inductance of HS inductor with m, n-turns spiral structure.

5. CONCLUSION

In this letter, a 3-D heterogeneous solenoid inductor based on TSV is proposed. By adding planar spiral structures at the ends of TSV, horizontal magnetic flux is introduced, and thus the inductance is promoted by more than 41%. Besides, an accurate analytical model of the proposed inductor is established which considers the position factors including offset and angle. Ansys Q3D simulation results show that the percentage error of the model is less than 5.38% for the parameters in usual cases. Thus, it can be used for quick and accurate estimation of turn number and area to be occupied. Moreover, the total inductance value can be fine-tuned by adjusting the number and turns of the planar spiral structure, which is conductive to the precise design of devices such as filters.

ACKNOWLEDGMENT

This work was supported the National Natural Science Foundation of China (62071282) and the Fundamental Research Program of Shanxi Province (202203021211295).

REFERENCES

1. Tida, U. R., V. Mittapalli, C. Zhuo, and Y. Shi, "'Green' on-chip inductors in three-dimensional integrated circuits," *2014 IEEE Computer Society Annual Symposium on VLSI*, 571–576, 2014, doi: 10.1109/ISVLSI.2014.117.
2. Tida, U. R., R. Yang, C. Zhuo, and Y. Shi, "On the efficacy of through-silicon-via inductors," *IEEE Trans. Very Large Scale Integr. (VLSI) Syst.*, Vol. 23, No. 7, 1322–1334, Jul. 2015.
3. Feng, Z., C. A. Bower, et al., "High-Q solenoidal inductive elements," *IEEE MTT-S Int. Microw. Symp. Dig.*, 1905–1908, 2007.
4. Zheng, J., D.-W. Wang, W.-S. Zhao, G. Wang, and W.-Y. Yin, "Modeling of TSV-based solenoid inductors for 3-D integration," *IEEE MTT-S Int. Microw. Symp. Dig.*, 1–3, Suzhou, China, Jul. 2015.
5. Wang, F. and N. Yu, "Simple and accurate inductance model of 3D inductor based on TSV," *Electron. Lett.*, Vol. 52, No. 21, 1815–1816, Oct. 2016.
6. Gou, S., G. Dong, Z. Mei, and Y. Yang, "Accurate inductance modeling of 3-D inductor based on TSV," *IEEE Micro. Wireless Compon. Lett.*, Vol. 28, No. 10, 900–902, Oct. 2018.
7. Xiong, W., G. Dong, Z. Zhu, and Y. Yang, "Compact and physics-based modeling of 3-D inductor based on through silicon via," *IEEE Electron Device Lett.*, Vol. 42, No. 10, 1559–1562, Oct. 2021, doi: 10.1109/LED.2021.3107320.
8. Mondal, S., S.-B. Cho, and B. C. Kim, "Modeling and crosstalk evaluation of 3-D TSV-based inductor with ground TSV shielding," *IEEE Trans. Very Large Scale Integr. (VLSI) Syst.*, Vol. 25, No. 1, 308–318, Jan. 2017.
9. Qu, C., Z. Zhu, Y. En, L. Wang, and X. Liu, "Area-efficient extended 3-D inductor based on TSV technology for RF applications," *IEEE Trans. Very Large Scale Integr. (VLSI) Syst.*, Vol. 29, No. 2, 287–296, Feb. 2021, doi: 10.1109/TVLSI.2020.3036385.
10. Paul, C. R., *Inductance: Loop and Partial*, 236–239, Wiley, New York, NY, USA, 2010.
11. Jayaraman, S. S., V. Vanukuru, D. Nair, and A. Chakravorty, "A scalable, broadband, and physics-based model for on-chip rectangular spiral inductors," *IEEE Trans. on Magn.*, Vol. 55, No. 9, 1–6, Sept. 2019, Art no. 8402006, doi: 10.1109/TMAG.2019.2916501.